2004

Patterning Polymer Thin Films: Lithographically Induced Self Assembly and Spinodal Dewetting

Regina C. Carns
Pomona College

Patterning Polymer Thin Films: Lithographically Induced Self Assembly and Spinodal Dewetting

Regina C. Carns

May 6, 2004

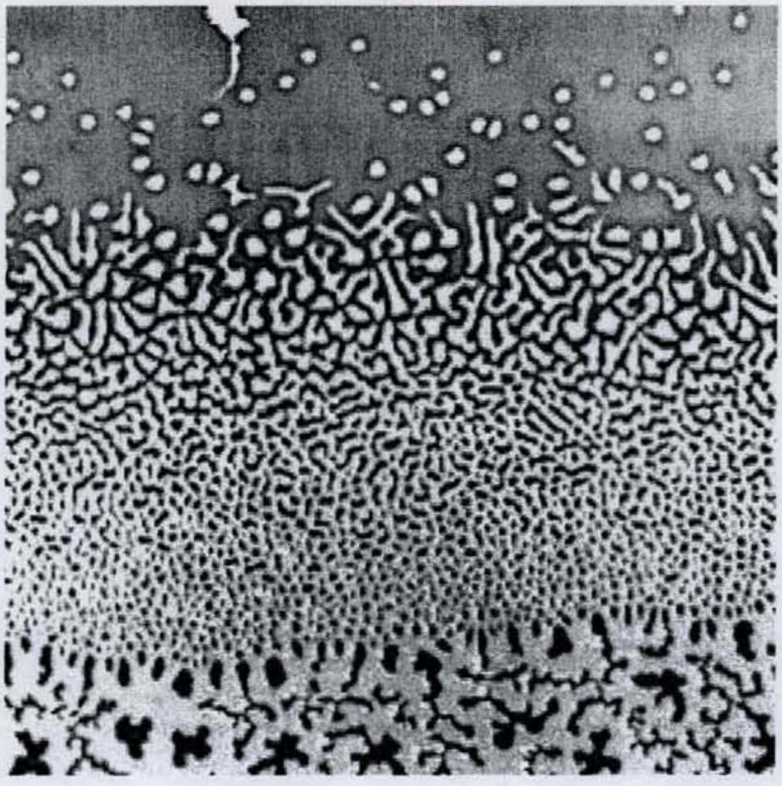

Acknowledgements

I wish to acknowledge and thank the many people who helped make this project a reality:

My thesis advisor Dr. David Tanenbaum, who was an absolutely indispensible source of theoretical information, contacts in the microlithography community, suggestions on lab technique, and general knowledge;

Glenn Flohr, who provided the assistance and equipment to create the pressure cell used in my experiments;

David Haley and Jeff Olivares for additional help with materials and equipment;

Brett Close and James McFarland for their atomic force microscopy skills;

Steven DeFord for the use and abuse of his server;

James and Teresa Carns, Adrienne Victor, Benjamin Hardy, Pamela Rettig and many others for general moral support;

And finally, much gratitude to the Motley coffeehouse for their quad-shot cappucinos, without which this thesis would not have been possible.

Contents

1 Introduction

Throughout the twentieth century, the field of electronics underwent a steady acceleration, moving quickly from huge, slow, astronomically expensive behemoths to small, quick, affordable home computers and an ever-increasing menagerie of other devices. Now, as these devices in turn start to become absurdly tiny and so cheap as to be disposable, the industry's mechanisms for creating ever-smaller devices and circuits are beginning to show signs of strain. The massive machinery of production is inadequate to its tasks, the designs run up against the barriers of basic physics, the expense skyrockets and the profits fail to increase.

In an age in which the microchip is ubiquitous, the rewards for novel methods of microfabrication are great, and the vast possibilities of nanotechnology lie just a little ahead. Various methods of microlithography offer differing benefits, and even as older techniques such as optical lithography are being refined beyond what were once considered their upper limits of resolution, new techniques show great promise for going even further once they reach their technological maturity. Recent developments in optical lithography may allow it to break the 100-nm limit even without resorting to x-rays; in the meantime, Steven Chou and associates have demonstrated successful replication of 25-nm features using imprint lithography [4]. The field is a vast and burgeoning one, with newer and smaller devices—usually for manipulating or storing data—being announced every week.

For forward-thinking inventors, however, these techniques are simply too cumbersome for the sub-micron machinery they hope will usher in a new era of nanotechnological marvels. Visionaries such as Eric Drexler imagine machines that create themselves out of nanometer-sized building blocks, taking advantage of atomic-scale interactions and the unique physics of the very, very small. Such complex assemblers are still firmly in the realm of vision, but simpler self-assembled materials are already an important part of micro- and nano-scale research. A symposium on self-assembled nanostructured materials held in San Francisco in April of 2003 attracted over 250 abstracts for posters and oral presentations [11].

2 Nanoimprint and Self Assembly: LISA

2.1 Imprint Lithography

In this fast-moving field of nanotechnology, any method that offers the possibility of smaller feature size or higher throughput attracts interest. Lithographically induced self-assembly is an outgrowth of the process of imprint lithography, a construction technique in which a mold is pressed into a layer of polymer to pattern it. Imprint lithography, not being dependent on the wavelength of light, is useful for the creation of particularly small feature sizes, in the tens of nanometers [3] Many products currently on the market incorporate the technique, most notably compact discs and DVDs [10] with micron-scale features imprinted in polycarbonate. For scientific purposes poly (methyl methacrylate), or PMMA, is the most commonly used imprintable material.

Imprint lithography has become a particularly attractive patterning technique as microchip feature sizes fall below the 100-nm threshold. Most techniques for patterning such small features are slow (serial techniques like e-beam lithography), or involve expensive and complex equipment (X-ray lithography), or both. Imprint lithography, however, is almost childishly simple in concept and basic theory, and nearly as easy to apply. Rather than being dependent on any form of energy beam, it depends on physical forces familiar to anyone who has ever made sugar cookies or entertained themselves with Play-Doh. It is startlingly successful; in experiments imprint-lithography masks have shown excellent reproduction capabilities and surprising durability, with none of the edge effects of optical lithography. Release agents added to the polymer before it is imprinted keep the mask from adhering, and heating the polymer above its glass transition temperature makes it soft enough to avoid any other damage. This durable re-usability means that this technique can be used with high throughput, both because of its re-usability and because of the potentially parallel nature of large or rolling masks.

Chou and colleagues demonstrated the possibilities of nanoimprint lithography by constructing a prototype "CD" that might hold 400 gigabits of information per square inch, using sub-10nm feature sizes [10]. Others have proposed that the technique be used in construction

of nanofluidic devices, transistors, and other nanoscale logic structures.

2.2 LISA: New Techniques

Lithographically induced self-assembly (LISA) appeared in the field of sub-micrometer fabrication about five years ago: Stephen Y. Chou and Lei Zhuang note in the abstract of their first paper on the subject, published in 1999, that they did not believe the effect had been previously observed [1]. Shortly thereafter Chou et al. published another paper on lithographically induced self-construction (LISC) a closely related procedure [2]. S. Y. Chou, L. Zhuang, and their colleagues at Princeton university are responsible for a significant portion of the extant literature on LISA and LISC.

Most other work on LISA has been published by an international collaboration, whose first paper on the subject appeared in 2001. Schäffer et al. replicated some of Princeton's observations and added others of their own, using somewhat different experimental techniques but achieving substantially similar results [13, 15]. Since its discovery, a wide variety of uses for LISA have been proposed; it might be able to achieve smaller feature sizes, to connect electronic parts after they are assembled on the macroscale, or to store data with high density. Suo and Liang note [17] that the effect could provide for finely tuned, programmable, rewritable storage mechanisms, perhaps using an array of AFM tips just above the polymer surface for fine control.

2.3 LISA: The Observed Phenomenon

LISA occurs when the mold or mask which would normally be pressed into the polymer is instead suspended a small distance above it (usually a few hundred nanometers.) Chou et al. actually discovered the phenomenon when dust particles in a contaminated imprint lithography sample acted as standoffs and kept the mask from making contact with the PMMA layer. In the presence of a few-hundred-nanometer gap, the polymer rises up to meet the mask, either in periodic pillar arrays (LISA) or mesas corresponding to features on the mask (LISC.) Although the effect was first observed using PMMA, a variety of different polymers may be used [15]. Interestingly, while Chou et al. succeeded in forming LISA and

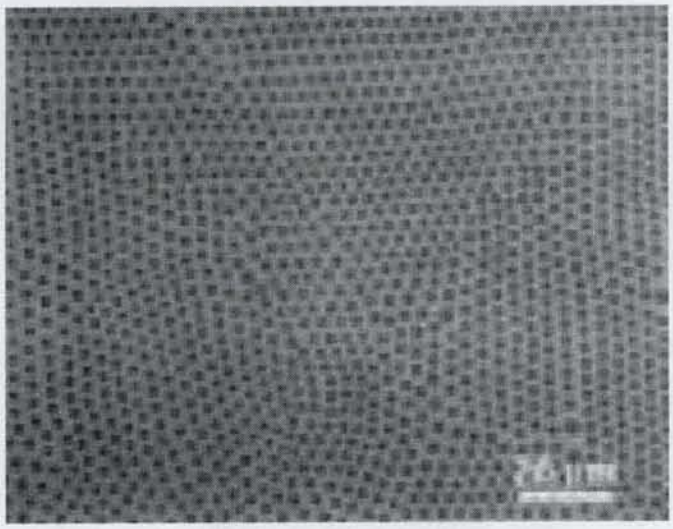

Figure 1: A regular lattice of pillars, showing a crystalline structure with variously oriented domains [1]

LISC through naturally generated electrostatic fields alone, Schäffer et al. were unable to achieve self-assembly without an externally applied electric field (generally between 20 and 50 volts.)

LISA may occur in a variety of forms, depending on what features may be present on the mask above it. The basic format is a geometrically regular array of pillars, whose size and arrangement are affected by the features on the mask above. If the features on the mask are more than 50nm in diameter, the crystalline structure may form domains of varying orientation. In large regions where the crystalline structure is not dominated by edge effects, the columns tend to form in a hexagonal closest packed structure [13].

Under some conditions, however, LISA may occur in relatively disordered forms. Chou et al. observed electrohydrodynamic destabilization at a liquid/liquid interface, for instance, and found that varying temperatures could drastically reduce or increase the orderliness of LISA structures [7]. The disorderliness in this case depended on both the temperature and the medium in which the polymer was immersed; somewhat different results appeared for air versus oil.

Chou et al. found that the presence of features on the upper mask affected the pillar formation, such that the pillars formed only underneath the protruding features and took on

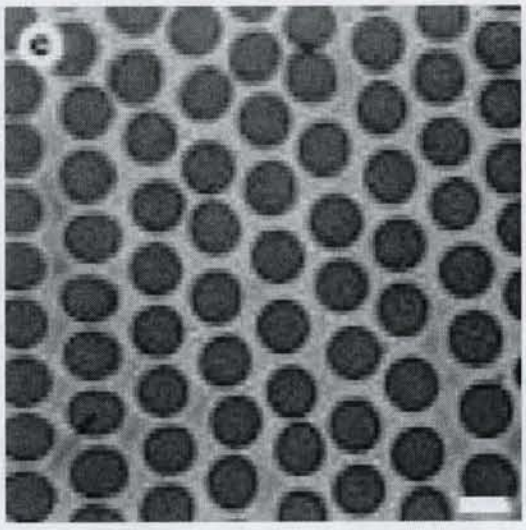

Figure 2: The characteristic hexagonal structure appears in Schäffer's work as well, although the image is too small to determine the existence of domains. [13]

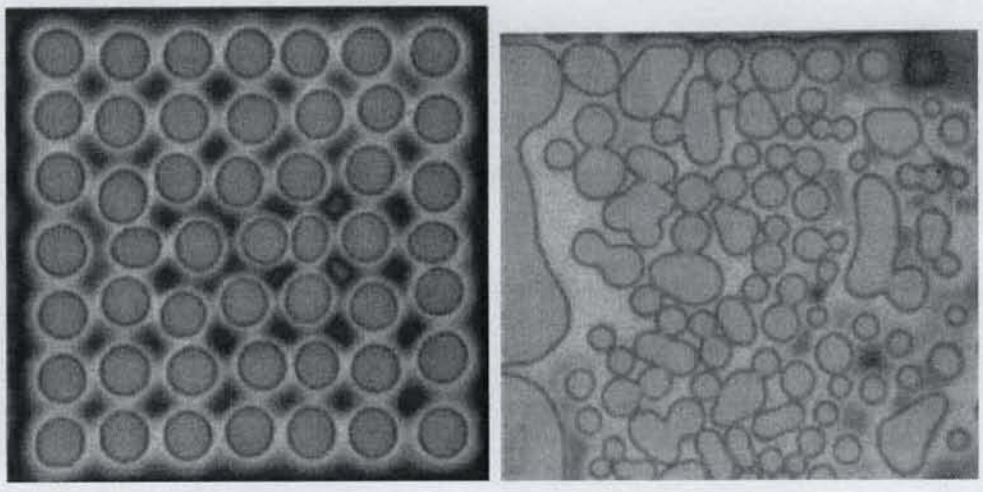

Figure 3: The first image is of LISA in air with a 9-minute heating at 135 degrees Celsius. The second was heated for 3 minutes at 160 degrees. [7]

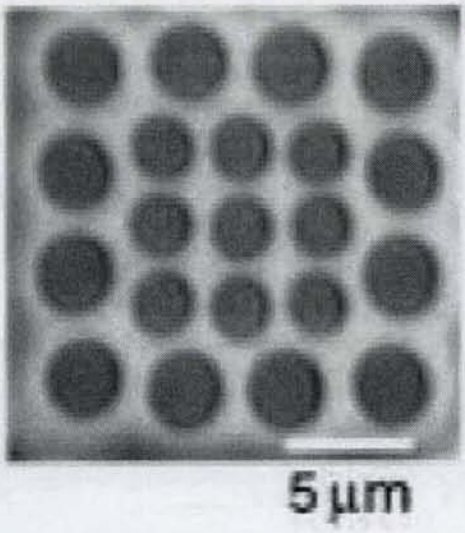

Figure 4: This image shows the pattern in which LISA pillars form under a square-shaped mask feature.[1]

an orderly form affected by the feature shape. Fig. 4 shows the effects of a square pattern on the upper mask; the usual hexagonal pattern and even feature size of the orderly LISA is superceded by the square pattern. In a later paper Chou et al. show that the corner pillars of such a structure form first, presumably because of the intensity of the electric field at these locations, and the rest of the structure is influenced by these initial pillars instead of taking on the more usual hexagonal formation [6].

The LISA formation can follow a variety of structures, from basic squares and triangles to this representation of the word "PRINCETON."

In each case edge effects dominate, ordering the pillar formations to correspond to the mask feature above.

Lithographically induced self construction (LISC) is substantially similar to LISA in basic theory and experimental technique; whether LISA or LISC forms on a particular sample depends on factors such as surface energy of the mask and feature size of any protruding

areas.

3 Mechanisms of Self-Assembly

The theory behind lithographically induced self assembly has been approached by several authors. Herminghaus discusses the instability of thin-film dielectrics [8] the year before the initial paper on LISA; after it is published, fellow Princeton researchers Suo and Liang approach the problem from the perspective of columnar formation in a two-phase dielectric [17]. However, the theory seems to be worked out in most specific detail by Chou's and Schäffer's groups themselves. Their theories of the LISA formation are substantially similar in overall form, including terms for air pressure, the effects of surface tension, the electric field on the polymer, and the intermolecular forces. Chou et al., in their paper on LISA modeling [18], add a nonlinearity to the surface tension term in the equation first expressed by Schäffer et al. Using this nonlinear equation, Chou et al. achieve strikingly accurate computer models of the LISA process, demonstrating the feature sizes, patterns, and wavelengths previously demonstrated in experiment.

The self-assembly is caused by the electric field between the mask and the polymer, which may be generated electrostatically or applied externally. This field generates hydrodynamic instabilities in the polymer, setting up undulations in the thin film. These are reinforced by their proximity to the charged upper surface, and eventually they reach the mask and begin to spread out across it. These effects are all moderated by the surface tension of the polymer, which works against the electrodynamic effects in its minimization of the surface area of the polymer. The interaction between the electrodynamic force, the surface tension of the polymer, and the energy of the mask determines the size and type of the pillars (and also determines whether they will merge and form into a LISC mesa.) The pillars are often relatively tall for their width; typical aspect ratios (height over width) are between 0.25 and 1 [1].

Schäffer et al. are the first to propose a detailed model for the pressures that lead to the instability of the polymer surface and the eventual formation of LISA structures. The basic

equation for the pressures on the polymer surface as given in Schäffer's paper [14] is

$$p = p_0 - \gamma \frac{\partial^2 h}{\partial x^2} + p_e(h) + p_{dis}(h) \tag{1}$$

In this equation, p is the total pressure on the surface. p_0 is the atmospheric pressure. h is the total thickness of the polymer; the second term describes the effects of surface tension on the system, and the fourth term represents intermolecular van der Waals forces. The third term is the electrical influence on the system, given by the expression

$$p_e = -\epsilon_0 \epsilon_p (\epsilon_p - 1) \frac{U^2}{\epsilon_p d - (\epsilon_p - 1)h} \tag{2}$$

where ϵ_0 and ϵ_p are the dielectrical constants for the air and the polymer, U is the voltage between the mask and substrate, and d is the mask-substrate spacing. This electrical force is responsible for the instability of the polymer and its eventual formation into pillars and mesas.

The characteristic wavelength of the system also falls naturally from this equation. Schäffer et al. calculate this wavelength to be

$$\lambda = 2\pi \sqrt{\frac{\gamma U}{\epsilon_0 \epsilon_p (\epsilon_p - 1)^2}} E_p^{-\frac{3}{2}} \tag{3}$$

Chou et al. proposed a very similar equation in their paper on dynamic modeling of LISA processes [18], but including a nonlinear surface tension term:

$$p = p_0 - \sigma \frac{\frac{\partial^2 h}{\partial x^2}}{(1 - \frac{\partial h}{\partial x})} + p_e + p_{dis} \tag{4}$$

This gives the rather more complicated formula for the system's intrinsic wavelength, but in basic theoretical form it is little different from Schäffer's model of the LISA process; there seems to be general agreement on the mechanisms behind LISA, although the mathematical formulations themselves may differ in detail.

4 Polymer Dewetting

In thin polymer films above the glass transition temperature, a uniform coating of even thickness may not be the most energetically favorable state. In this case, depending on the wettability of the substrate, the polymer may begin to dewet. This process is observed in a wide variety of different types of thin films, including molten metallic films and liquid crystals. The initial surface rupture may occur, in metastable substances, due to nucleation by surface defects or impurities (heterogeneous nucleation) or spontaneous nucleation (homogeneous nucleation.) These substances require a high activation energy to begin the process of dewetting/phase separation. In unstable polymers, no such activation energy is necessary; minute fluctuations initiate the phase separation. This process, by which existing thermal fluctuations are amplified into characteristic patterns of dewetting, is called spinodal decomposition or spinodal dewetting.

Dewetting occurs when the second derivative of the free energy function with respect to concentration (or height) becomes negative, and it becomes chemically favorable for fluids to flow from areas of lower concentration to areas of higher concentration. Jones gives the equation

$$F = A \int [f_0(\phi) + \kappa(\frac{d\phi}{dx})^2]dx \tag{5}$$

for the total free energy of the system, where A is the area, ϕ represents the composition of the material and $f_0(\phi)$ the free energy with respect to composition, and κ is a coefficient specific to the material being studied called the gradient energy coefficient. [19] Jones notes that this equation applies to a wide variety of materials.

The fact that this equation is formulated to be dependent on compositional fluctuations reflects the dominance of mixtures in the study of spinodal dewetting, which is more characteristically observed in the case of polymer blends or copolymers and which therefore represents a true phase separation. In the case of homopolymers and other uniform substances, we find that height fluctations take the place of compositional fluctuations in this equation in determining the free energy of the substance.

The spinodal decomposition process is differentiated from LISA by its disordered character. Whereas LISA develops in regular, periodic arrays as a result of the imposed electric field, spinodal decomposition is essentially random, developing as it does from thermally induced capillary waves at the polymer surface. Spinodal decomposition *does*, however, demonstrate a characteristic length scale, making it a very distinctive phenomenon. The characteristic wavelength of spinodal decomposition occurs at the equilibrium between long wavelengths, where the distances between peaks and troughs become too large for quick diffusion, and short wavelengths where the free energy is significantly affected by the greatly increased surface roughness/surface area [19].

5 Procedural Considerations

The initial version of the experimental procedure follows principally from S.Y. Chou and L. Zhuang's first paper on lithographically induced self assembly, in which they describe the fundamental format of the process [1]. The basic components of lithographically induced self assembly are a substrate coated with a layer of polymer on the order of 100 nm thick; and a mask, suspended above the polymer by a spacer, usually several hundred nm tall. The materials for each of these items, and the manner of their combination, may vary considerably from experiment to experiment.

5.1 Polymer: Composition and Deposition

The exact type of polymer used does not seem to have a strong qualitative effect on the self-assembly phenomenon. Schäffer et. al. performed the experiment with polystyrene, brominated polystyrene, and polymethylmethacrylate; this range of polymers is in contrast to S. Y. Chou et. al. who used only the latter, PMMA. The distinction between the different polymers is principally evident in their differing dielectric constants, which result in varying characteristic periods of pillar spacing. A higher ϵ_p results in a smaller spacing, since the electrostatic force is more easily able to overcome the surface tension. This is consistent with the predictions of the characteristic wavelength equation (3) derived by Schäffer et al.

Spin-coating the chosen polymer onto the substrate provides a smooth, even layer of polymer, and varying the composition of the polymer and the angular speed of spin can control the thickness of this layer. For most applications requiring a polymer layer on the nanometer or micron scale, it seems to be the preferred method. Previous experiments [1, 2, 13, 14, 15] using thicknesses between 90 and 200 nm, found that the LISA phenomenon is not very sensitive to polymer thickness.

5.2 Mask and Standoffs

The mask or top plate in the LISA/LISC process is of some importance to the behavior of the liquefied polymer, insofar as it affects the behavior of the electric field—induced or electrostatic—between the mask and the polymer/substrate. Typically the mask is made of silicon coated with a self-assembled monolayer such as octadecyltrichlorosilane to facilitate removal of the polymer after the heating cycle. A pattern may be etched into the mask or into a silicon dioxide layer on its surface, or it may be added in another material with different conductivity and surfactant properties. In some cases, to improve the function of the mask as an electrode, Schäffer et al. coated the back with a thin gold layer. For experiments in which it is considered desirable that the mask be transparent, such as the observation of the dynamic properties of LISA formation, an Indium-Tin-Oxide (ITO)-coated microscope slide may be used instead.

In general, the exact properties of the mask do not seem to strongly affect the LISA formations, except insofar as LISA pillars or LISC mesas will closely follow any protrusions on the mask. The mask can also be used to provide a substrate for thin evaporated-metal rails, some hundreds of nanometers high, to act as standoffs and maintain the appropriate separation between mask and polymer. Chou and colleagues favored this method and used it to achieve a uniform mask-polymer distance across the samples. Schäffer et al., favoring a "wedge" geometry that provided a wide range of distance regimes, and needing a non-conductive standoff, used a "step" etched into the silicon itself. Another possible standoff mechanism, inspired by the dust particles that initially brought the LISA phenomenon to the attention of S. Y. Chou and colleagues, might involve colloids of the appropriate particle

diameter scattered across the mask or polymer.

6 Carrying Out the Process

6.1 Preparation of Substrate

In this experiment, the substrate is silicon wafer. This wafer is reduced to pieces of a manageable size (generally between one and two inches across, in order to provide adequate workable area and still fit into the pressure cell) by scoring it along a straight line using a diamond scribe and then applying pressure on either side to break it along the scored line. This process scatters some tiny fragments of silicon across the wafer surface from the scoring, but alternate procedures tend simply to shatter the wafer into unusably small pieces. In later runs, having become more adept at the manipulation of the silicon wafers, I found that inscribing a small scratch on the edge of the wafer was often sufficient to make it cleave cleanly with applied pressure. This method did produce slightly more bad breaks, but when it worked correctly it generally resulted in a straighter break and a cleaner substrate.

Cleaning the substrate was a difficult process as well, and eventually I settled upon a repeated cycle of acetone followed by isopropyl alcohol and dried with KimWipes. Due to a lab shortage of acetone, some wafers were cleaned with only isopropyl; this did not seem to make a noticeable difference in results. The substrate received another acetone/alcohol rinse during its initial spin in the spin-coating apparatus. The spinning apparatus consisted of a flat metal plate driven by the food processor's motor. A hole in the middle connected to a small fishtank pump, creating a vacuum chuck. A small O-ring coated with vacuum grease sat between the substrate wafer and the metal platform to improve the vacuum's hold on the wafers under high spin.

The substrate shape proved to be somewhat significant in the spin process, as asymmetrical substrate wafers sometimes flew off the spin apparatus despite the assistance of the vacuum chuck. Once the substrate was clean and had demonstrated its ability to stay in place under spin, I transferred a quantity of 50% polymethylmethacrylate (molecular weight 495 K) diluted with anisole onto the substrate and turned on the spin apparatus for one minute.

Generally the polymer reached its final thickness quickly, changing color as it grew thinner and its thin-film reflective properties changed until it reached a final, relatively uniform light yellow/gold color, shading to light blue after it was baked. This optical property of the thin film proved useful, insofar as it provided a rough optical indication of the film thickness. Once spun for 60 s and baked at 70-80 degrees Celsius for 60 s, the polymer-coated substrate was ready for use.

The polymer substrates generally demonstrated a variety of imperfections, incompletely covered edges, dust particles, and the like. These might have been eliminated with more elaborate cleaning mechanisms, but they also served to provide visual landmarks and additional standoffs (for some time, Dr. Tanenbaum and I theorized that the dust particles on the polymer substrate were in fact more important standoffs than the aluminum layers that had actually been intended for that purpose.)

Using the Pomona physics department ellipsometer, we found the thickness of the polymer varied by about 5-10 nm across the surface of a single sample and ranged from 158 to 180 nm on all samples. Given the relatively imprecise sample preparation techniques, this range was entirely acceptable; considered as quarter-wavelengths, these measurements are also consistent with the observed coloration of the plates.

6.2 Preparation of Mask

To create the necessary gap between the mask and the lower plate, I determined to use a wedge geometry, with one standoff/step partway along the mask. Initially, I used a 100nm gold colloid for this purpose, dripping a small amount of the colloid on one end of the upper plate, attempting to encourage clumping so that the standoff might reach several hundred nanometers in height. For subsequent trials, however, I abandoned this method in favor of the more controllable evaporated metal standoffs.

To construct a standoff of the proper height, I used the metal-evaporating apparatus to deposit aluminum on the surface, covering a portion of the plate with a piece of tape or aluminum foil so that a well-defined line would be left behind when it was removed.

The metal-evaporating apparatus consists of a large bell jar that is evacuated to approxi-

mately 10^{-7} torr using a rough-pump vacuum and a He Cryogenic Pump. It contains two sets of electrodes between which I placed tungsten "boats" carrying pellets of aluminum. Once the jar was evacuated, these boats could be heated with 140-160 A of current in order to melt and vaporize the aluminum. A large metal canister protects the interior of the bell jar from being coated with the vaporized aluminum, and at the top of this canister is an opening over which the samples may be placed.

In order to achieve greater thickness. I constructed a wire holder in which I could place silicon plates halfway down the inside of the canister. Theoretically, by inverse-square laws, one would expect this to approximately quadruple the aluminum they collected, although in practice it seemed to be slightly less effective. Generally it took several "boats" of aluminum in order to approach the needed thickness of deposited metal. The first run deposited 330nm of aluminum as measured by Brett Close on the AFM. The second and third runs proved more difficult to measure accurately due to a slightly gentler slope, but eventually I determined their heights to be approximately 260 nm and 280 nm, respectively. In each run, I also placed a few silicon wafers on the top of the canister (at the normal height) although I did not use these in experiments due to the small thickness of deposited aluminum.

6.3 Experimental Conditions

Once the lower plate was coated with polymer and the upper with its aluminum standoff, I placed them face to face. Previous experiments in LISA used a high pressure to ensure good contact between the two plates. Locating a mechanism that could both produce this pressure and supply heat to the samples, particularly in such a way that it could be controlled and measured, posed something of a challenge. Initially I attempted to create pressure using simple weights placed atop the silicon wafers as they baked on the hot plate. These, however, proved entirely inadequate to the purpose.

Dr. Tanenbaum and Glenn Flohr helped me to arrive at a design for a device that could exert a high pressure and allow for this pressure to be monitored with relative precision, and which was sufficiently small and heatproof that it could be placed on the hotplate in Dr. Tanenbaum's lab. The device, constructed of machined aluminum, consists of a sealed metal

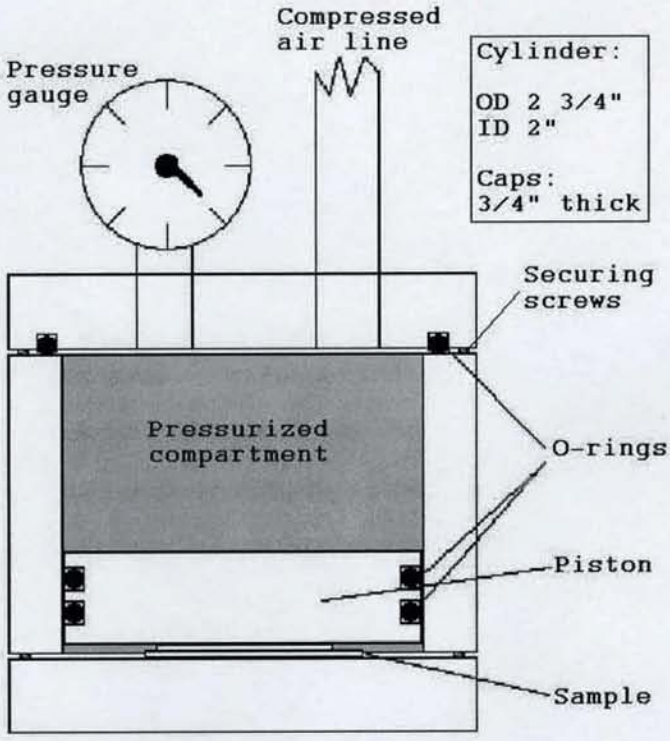

Figure 5: The device I constructed to exert pressure on the samples.

cell with a piston; the valve on the top connects to a compressed-air line or pressurized gas cylinder, and this pressure in the top portion of the cell pushes the piston downwards to in turn exert pressure on the sample. (See Figure 5.)

The construction of this device to appropriate tolerances took me approximately three weeks. The sides of the piston and the O-rings are coated in vacuum grease to provide both lubrication and an airtight seal.

Once this device was constructed, I placed the silicon wafers in the location indicated in the diagram, connected the device to the building's compressed air lines, and turned on the air. The air lines proved to contain a certain amount of water, and in subsequent runs I always made sure to blow this out before beginning (although failing to do so would probably not have adversely affected the apparatus, which was presumably watertight when pressurized.) Placed on a hotplate pre-heated to the appropriate temperature, the device reached thermal equilibrium in 30 to 45 minutes.

I used several different temperatures from 120 to 165 degrees Celsius, although the diffi-

culty in controlling other variables made it difficult to be certain how much the temperature affected the final polymer forms. During later runs I used a thermocouple provided by Jeff Olivares, with the probe sandwiched between the bottom cap and the body of the device, to measure the approximate real temperature reached by the silicon plates. This temperature proved to be generally ten to twenty degrees Celsius below the temperature recorded by the hotplate: for 160-165 degrees, it was about 140; for 130 degrees, about 115; for 120 degrees, about 110.

In order to ensure adequate time for the polymer to heat, all runs extended for at least two hours. Chou et al. noted that the exact amount of heating time did not seem to affect the outcome, so the uncertainty inherent in bringing the entire device to thermal equilibrium with the hotplate did not concern me overmuch, and my results gave no indication that it was an issue. After an adequate interval, I turned off the hotplate and allowed the device to cool before turning off the air pressure, carefully relieving the accumulated pressure within the device, and removing the silicon wafers.

The pressure of the compressed air line varied somewhat over time, changing unpredictably between 75 and 85 PSI, but this relatively small variation seemed unlikely to affect the results significantly. In particular, the piston was closely fitted and stiff, the silicon samples rather inelastic; the system probably would not move in response to such small fluctuations in pressure.

6.4 Imaging of Completed Plates

The optical microscope proved to have insufficient resolving power to observe the micron-scale structures of LISA. The atomic force microscope, however, gave excellent images and also permitted close measurement of feature size and height. The AFM in Professor Tanenbaum's lab is housed in a vibration-proofed chamber containing a movable, rotating platform for samples; this platform incorporates a vacuum chuck to keep samples from moving while they are imaged. I used it in tapping mode exclusively. Since I sought features on the order of a few microns in diameter, I generally set the scan to a few tens of microns across, with a scan rate, gain, and resolution determined via trial and error for the particular features of

each sample. Too fast a scan rate tended to cause "streaking", too much gain could cause uncontrolled oscillation of the tip, and so on.

After examining the first few PMMA plates, I found that the patterning of the polymer showed a distinctive roughened appearance on a macroscopic scale, permitting me to locate areas of pattern easily and to determine almost immediately whether a particular run had successfully created patterned spots in the PMMA. Since the areas of patterning appeared relatively random, I did not develop any particularly methodical way to image each area; I simply tried to image at least a few patterned areas on each plate, and took additional images of patterns that struck me as particularly interesting or novel.

The NanoScope IIIa software (version 4.43r8, made by Digital Instruments) includes a wide variety of image analysis and manipulation tools. These allowed me to analyze the images with a great deal of precision and detail, with the ability to cross-section the image heights proving particularly useful, along with the two-dimensional Fourier power spectrum analysis that provided an idea of the natural periodicity of the samples.

7 Results

7.1 Patterns: Qualitative

Since the masks I used were flat and unfeatured, I looked for the periodic pillars of LISA rather than the mask-shaped features of LISC. Patterned areas demonstrated a characteristic roughened and darkened appearance in the optical microscope, with larger patterns often individually visible.

The first specimen I examined in detail was the polymer-coated plate from the first run. Curiously, although I found features of roughly the right size and shape, they were concave instead of convex. This initially suggested to myself and Dr. Tanenbaum that the pillars had in fact formed as expected, but adhered to the mask when the two pieces were separated—leaving inverted images of themselves in the polymer of the base plate.

AFM observation of the mask suggested that this was indeed the case. Pillars of varying sizes and levels of organization appeared on the mask near the metal standoffs. However,

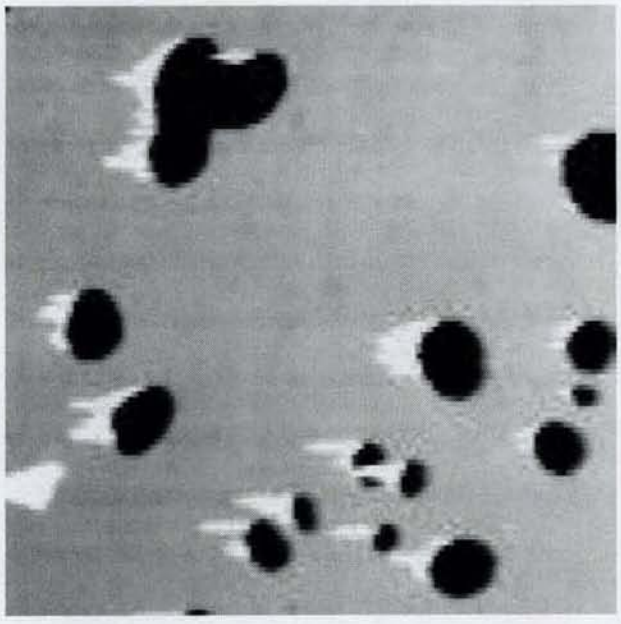

Figure 6: Holes in the base plate of the first run. This image is 10 μm across.

later examination of other plates, and further examination of the plates from the first run, showed that this initial theory was incorrect; the holes appeared to be a natural result of the self-assembly processes occurring on the plates, not a result of pillars forming and adhering to the mask. Whether the features that *did* appear on the masks formed on the base plate and then stuck to the masks as they pulled away, or perhaps formed on the masks in the first place by some other mechanism, is still open to speculation. Because of the small feature size, it is impossible to identify which areas of a particular mask exactly opposed a particular patterned area on the corresponding polymer-coated plate.

One frustrating aspect of the image analysis was the impossibility of empirically determining the exact distance between the mask and the substrate. For some samples, the flattened character of the features suggested that they had come in contact with the upper mask and spread out against it, allowing me to infer a rough estimate of mask-substrate separation from the feature height. However, because I could not be certain how much polymer lay below a particular feature, this method could not be considered exact. Although the height of the metal standoffs might be measured using the atomic force microscope, the wedge geometry of most of the samples, along with the difficulty in determining how far the standoff might

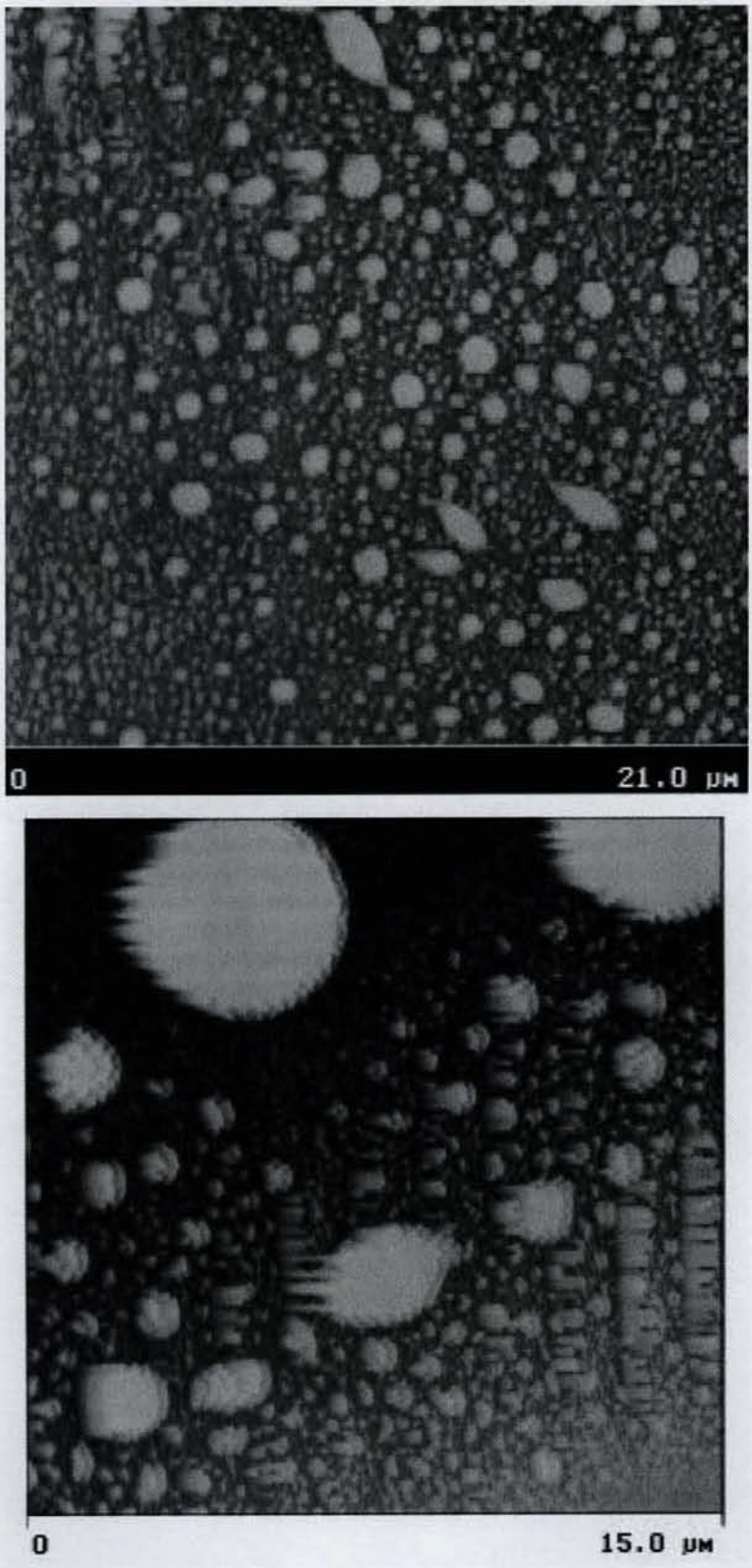

Figure 7: In these images, of the top plate/mask used in the first run, we see pillars of a variety of sizes. They are relatively round, however, and in some places even show traces of periodicity and hexagonal organization.

have embedded itself into the polymer surface, made it difficult to find the exact separation between the silicon substrate and the mask.

Indeed, the metal standoffs in some cases appeared to be relatively ineffective, with dust particles or impurities serving as the standoff instead, and self-assembled patterns forming around these. In order to test this theory, I ran one experiment with the usual polymer but a plain mask—no standoffs of any sort, only such particles of dust and fragments of silicon as might have collected on it incidentally. This run showed no notable self-assembly, suggesting that indeed the standoffs serve an important purpose and some minimal separation between mask and substrate is required for the observed phenomena to occur.

A wide variety of different self-assembled forms appeared on the various samples, showing no obvious relation to the experimental parameters. In most cases, particularly with high-temperature runs, they remained on the lower polymer sample; in a few cases they adhered to the mask. The forms fell into several categories: round holes, irregular holes, negative "labyrinths" and positive "labyrinths", and, on occasion, pillars.

7.2 Spinodal Dewetting

The labyrinths seem to be the most common pattern of self-assembly. Upon close examination, they demonstrate interestingly consistent properties; the "arms" of the patterns are more often than not all the same width, suggesting initially that these patterns formed through the partial merging of regular pillar arrays like those seem in ordered LISA. The labyrinth arms show a characteristic width that remains relatively consistent from sample to sample, varying from slightly less than one μm to about 1.5 μm (see Fig. 17 for a more quantitative analysis.) It seems reasonable to suppose that the width of the labyrinth arms is related to the characteristic LISA wavelength derived in various models of the process.

Near the end of the semester, however, I stumbled across a picture of a polymer that had undergone spinodal dewetting (Fig. 10) and immediately recognized the characteristic labyrinth features that had grown so familiar to me over the course of my long hours imaging in the lab. Further research indicated that these types of patterns are characteristic of processes in diblock and triblock copolymers, but may also occur in homopolymers such as PMMA.

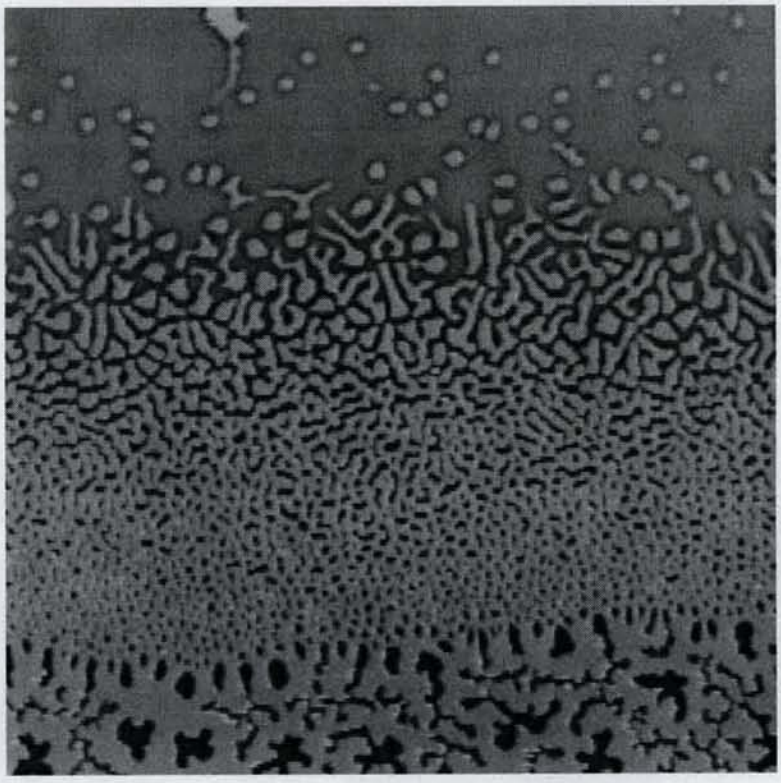

Figure 8: This image shows most of the patterns observed over the course of the experiments, all within an 80 μm square. Near the bottom are large, irregular holes and some hints of "negative" labyrinths; in the middle are arrays of small, roundish holes which grow and merge to create "positive" labyrinth-like structures; and at the top are scattered, isolated pillars. The image also demonstrates the quick transitions between structures that the polymer often displayed.

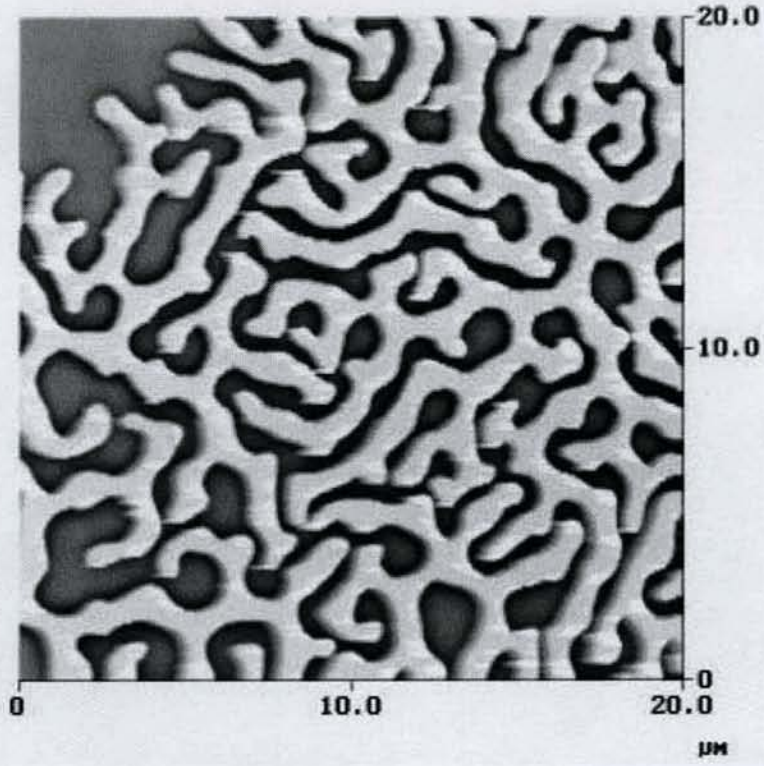

Figure 9: A characteristic positive labyrinth.

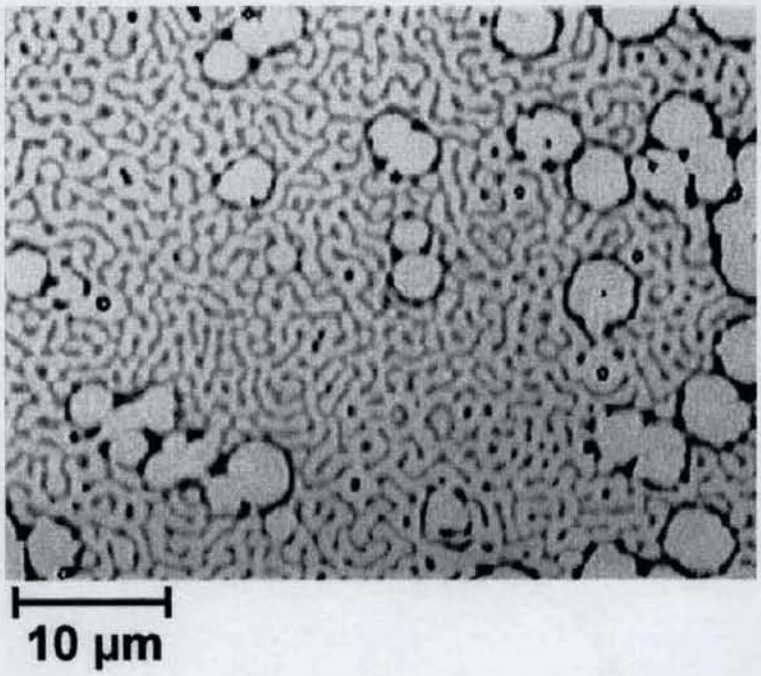

Figure 10: Spinodal dewetting. [12]

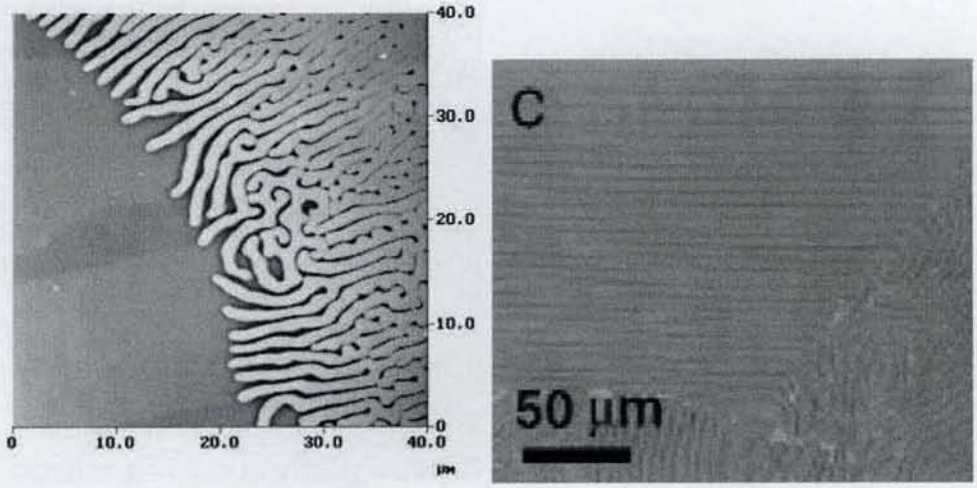

Figure 11: A partially aligned labyrinth from one of my samples, alongside Schift's orderly labyrinths.

This and other dewetting patterns [12] seemed to account for most of the observed structures on my samples, suggesting that perhaps the mechanisms of LISA had relatively little to do with my results. However, some areas exhibited a degree of orderedness uncharacteristic of spinodal dewetting, which is an essentially random process (although, like LISA, it does display a characteristic "wavelength.")

These competing explanations for the polymer features on my samples may not be mutually incompatible. Schift et al., examining the behavior of PMMA during imprinting, observed ordered labyrinths that seem to incorporate both the characteristic forms of spinodal dewetting and the orderliness, moderated by mask features, observed in LISA and LISC. Although my sample in Fig. 11 does not demonstrate the near-complete orderedness of Schift's, it does display a certain organization. It does not seem entirely impossible that it might represent some degree of ordered self-assembly.

Although spinodal dewetting seems to account for most of the forms I observed, the transition between patterns is still somewhat mysterious. In some patterns, it seems relatively clear that these pillars and labyrinth arms gradually merged into other forms. In others, however, the transition from one pattern type to another is sudden and difficult to explain. Given the conformation of the patterned areas, one possible explanation is that the patterns are affected by minute differences in the distance between the PMMA surface and the mask,

and that these differences are responsible for the transitions from unpatterned to patterned and from one type of pattern to another. The patterned areas tend to occur as loops or U-shaped regions, perhaps forming around impurities and defects in the substrate that create the appropriate conditions for pattern formation at a certain radius from the impurity.

Some work on thin-film polymer dewetting also suggests that the method of cleaning the underlying silicon substrate may have substantial effects on the patterns formed by the polymer. Different cleaning agents, for instance, may affect the breakup of the surface, and wiping with a Kimwipe apparently has a very significant effect on the nucleation and growth of surface irregularities [12].

7.3 Quantitative: Fourier Analysis and Heights

Because of my uncertainty as to whether the processes I observed were a result of lithographically induced self assembly or of more standard polymer dewetting processes, I did not feel confident in concluding that the height of the observed features necessarily represented the distance between the substrate and the mask. The flat upper surface of many samples does suggest that the polymer features often reached the up to the mask, whatever the exact mechanism of their formation. (Fig. 13)

The NanoScope program provided a wide variety of modes for numerical analysis and manipulation of captured images. The most useful of these for determining the height of individual features proved to be the cross-sectioning function, which provided profiles that might then be more carefully analyzed. The heights of features compared to the surrounding polymer substrate could provide an important clue to the mechanism of formation, since the pillars in LISA actually draw polymer from around their bases in order to reach upward to the mask. Unfortunately, since the behavior of spinodal dewetting under an upper mask is relatively unknown, this method could not definitively distinguish between the two possible mechanisms of feature formation but it might be considered to give a useful clue as to the degree of lithographically induced self assembly present in the samples.

In height analysis, some samples proved to be quite flat, with features appearing as undulations in the background polymer rather than rising above it. Fig 12 shows one such sample,

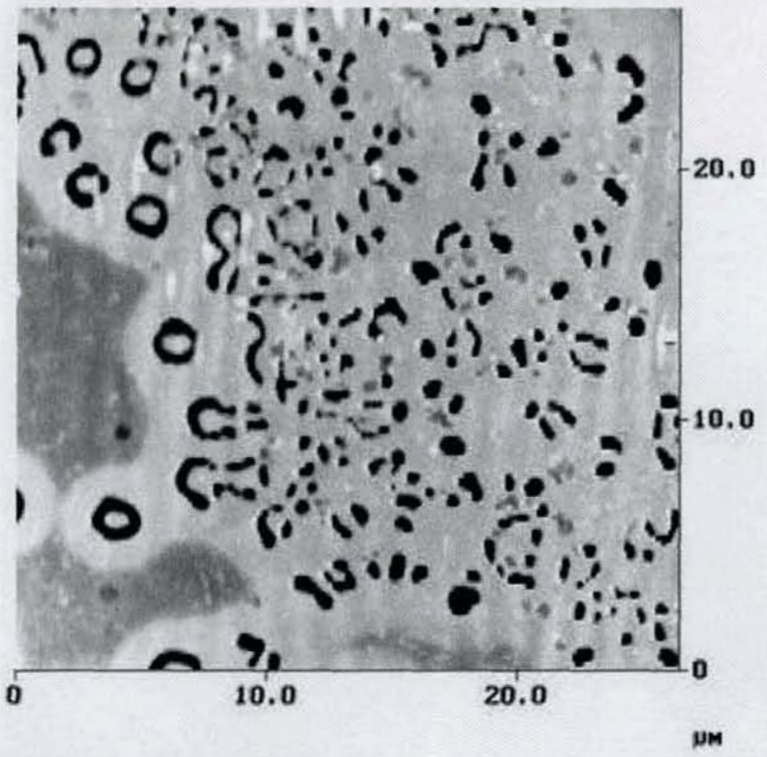

Figure 12: An area of polymer in which patterns sank into the surface instead of rising above it, creating a uniformly flat area with hole-like features

in which pillars create holes around themselves rather than rising up above the surrounding polymer layer. Other samples showed quite obvious pillar formation, with distinct pillars on flat planes (see cross-sections Fig 14 and Fig 15.) Fig 15, in particular, demonstrates the height and aspect ratio most typical of LISA pillars observed by other researchers. None of these samples, however, showed strong LISA periodicity.

Since both LISA and spinodal dewetting exhibit characteristic length patterns, I used the power spectrum analysis feature of the NanoScope program to determine whether any such characteristic wavelength appeared in my samples. Choosing images that displayed the same type of pattern over their entire area, I performed 2D spectrum analysis and found that the features did indeed display characteristic wavelengths, although these varied somewhat from sample to sample. The labyrinths generally showed moderate peaks between 1.4 and 2 μm wavelength; presumably the variance is due to the differing conditions present on different samples—and, indeed, on different areas of the same sample.

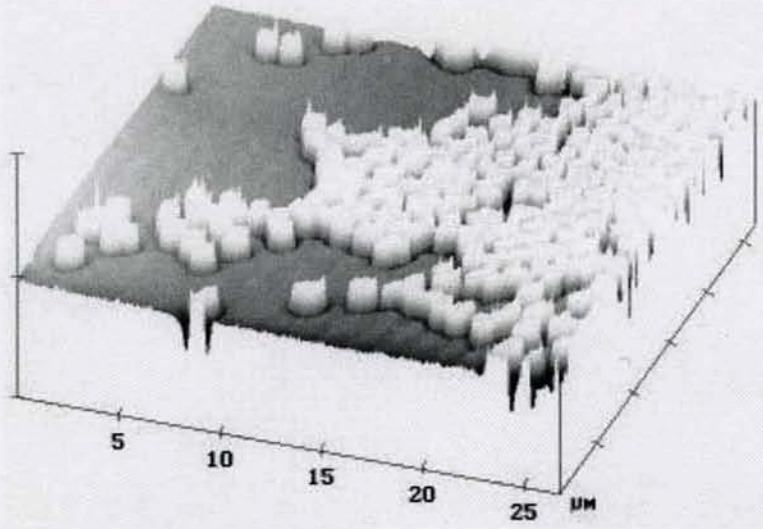

Figure 13: This three-dimensional representation of the features on one of the plates suggests that they were flattened by contact with the upper mask (the small, sharp spikes on the edges of the pillars are natural artifacts of AFM imaging.) Note also that the pillars draw polymer from around their bases, creating a sort of "pillar in a hole."

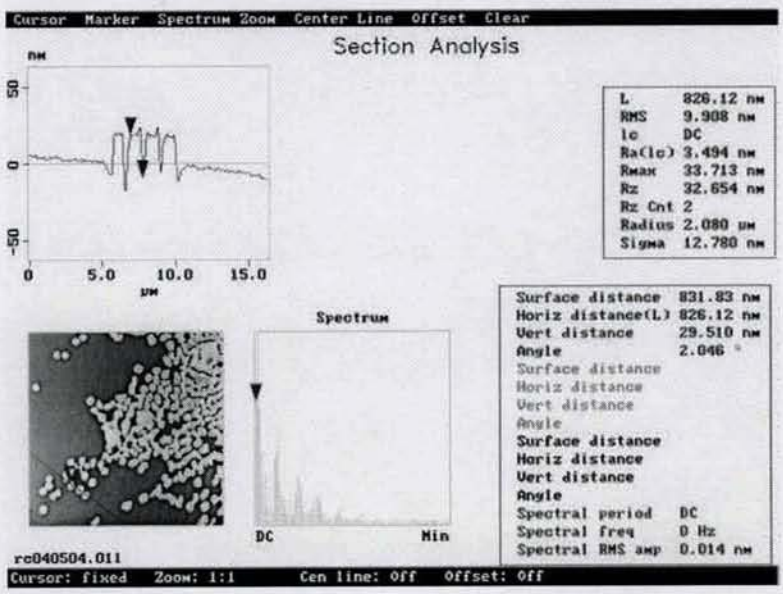

Figure 14: Pillars which reach above the surface around them. Note the small depressions in which they stand.

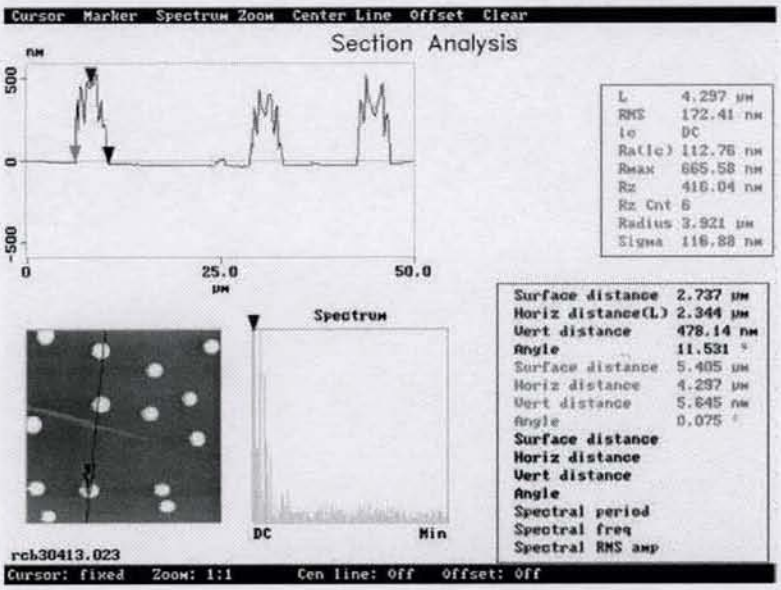

Figure 15: These pillars display an aspect ratio, shape and height typical of LISA, but not the close-packed periodicity usually associated with the phenomenon.

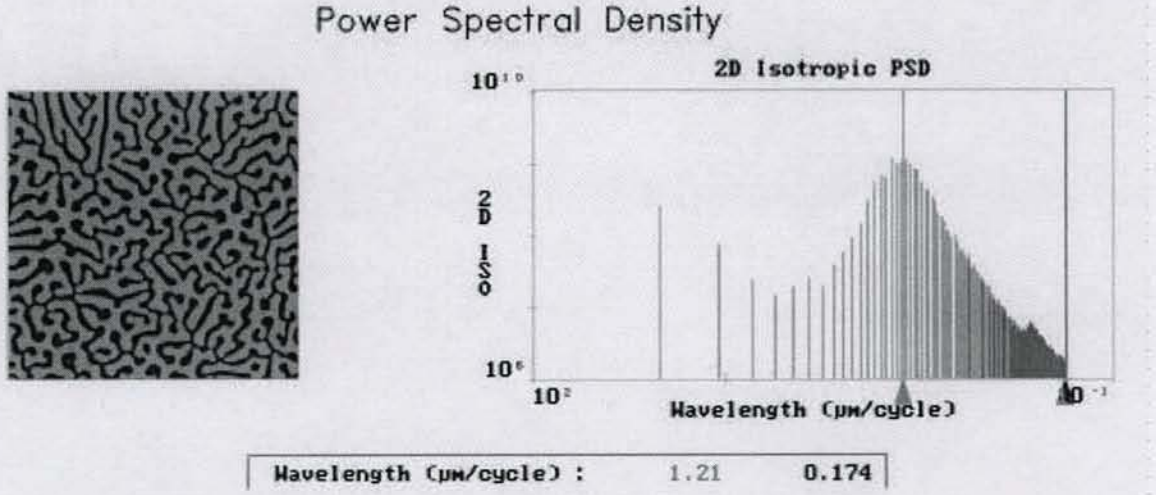

Figure 16: A single 2d power spectrum analysis, showing a particularly distinct peak at its characteristic length scale.

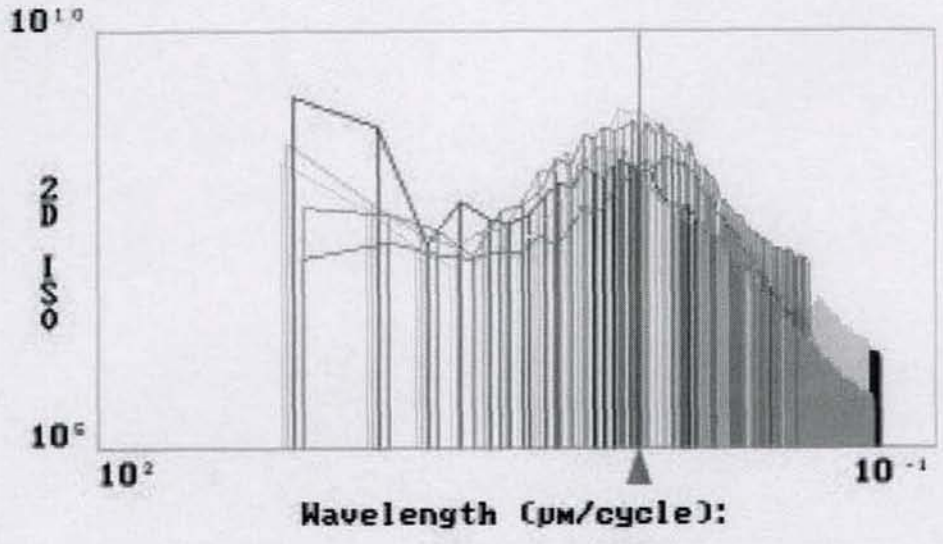

Figure 17: Several power spectra from various samples, showing the peaks around 1.4 μm.

8 Final Assessment and Potential for Further Research

The project may be considered a qualified success. Self-assembly in several different forms occurred in the experimental samples. The periodic, ordered pillars characteristic of LISA, however, did not appear in any of the samples. Where pillar arrays did form, they tended to be relatively chaotic, appearing in wide variety of sizes and with no clear mode of organization. Other patterns observed included positive and negative "labyrinths", irregularly sized and shaped holes, regularly sized round holes, and widely dispersed pillars or "stick-men" features. The "positive labyrinths" tended to show the most order of all the observed patterns, with "arms" of strikingly consistent width. They seem to represent a middle ground between LISA and LISC, with the pillars partially merged into "arms" but maintaining separation between the arms themselves.

The most likely mechanism for the formation of the observed features, based on examination of figures in various papers on polymer thin films, is that they are a result of spinodal dewetting. The "labyrinths", in particular, are extremely characteristic of this self-assembly process. Spinodal dewetting has some similarities to LISA in its essential mechanism and its exhibition of periodicity, but unlike LISA tends to create essentially random features. It is also possible that the observed results represent a relatively novel middle ground between

LISA and spinodal dewetting, as they display occasional signs of an organization which is uncharacteristic of basic spinodal decomposition.

Further study might include a number of variations on the basic experimental technique. Refinement of the existing techniques, obviously, might produce better results. Cleaning the silicon wafers more thoroughly, using a more sophisticated spinner to achieve a more even and consistent surface, and finding methods to more precisely control the heat and pressure might all improve the repeatability and clarity of the results. The standoffs, too, could be refined. Unfortunately I was not able to obtain silica colloid of the proper sizes to act as standoffs for this experiment; $.25\mu m$, $.50\mu m$, and $1\mu m$ colloids might have made convenient and highly consistent standoffs and provided more regular results. Combining more precise standoffs with superior cleaning techniques might permit a much more quantitative analysis of the effects of the gap between the mask and substrate.

The most obvious experimental change would be to add an externally imposed electric field, like that used by Schäffer and colleagues in their LISA experiments, or to somehow increase the insulation between the Si plates to ensure that a net electrostatic charge could be maintained between them. Dr. Tanenbaum and I worked out some plans for this part of the experiment, using Si wafers coated with oxide so that the conductive standoffs would not short circuit the potential across the wafers. The oxide could be etched off of a small area of the wafers, and fine wires attached using conductive paint, such that the entire assembly could still be fit into the pressure device. The wires might then be attached to a power supply that could provide 20 or 30 volts of DC current. Maintaining the appropriate insulation inside the aluminum pressure cell would require some ingenuity, but should not be extremely difficult. Thickly oxide-coated plates might also prove sufficient to create a more insulated system and encourage the spontaneous formation of a potential difference between the Si wafers, particularly in combination with nonconducting standoffs if such could be created or obtained.

Other procedural ideas came under consideration during the semester but never found time for implementation. Coating the mask with octadecyltrichlorosilane (OTS), a self-assembled monolayer, would have ensured that the pillars remained on the lower polymer substrate in-

stead of adhering to the mask, as they sometimes did on the bare silicon/aluminum. The process of applying the OTS, however, is a delicate and requires a dry box. Since the occasional adhesion of the polymers to the upper surface did not prevent analysis of data, and since the construction of the pressure device took up a significant portion of the semester, coating the mask with OTS did not seem to be a productive use of time.

The field of thin-film polymers and the microfabrication industry may not yet be ready for lithographically induced self asembly—or LISA may not be ready for it, being still in its relative infancy as a patterning tool. Nor has spinodal dewetting, with its attractive but chaotic formations, found any industrial use. These microscale phenomena still need characterization, control, and further research into their basic mechanims and their potential benefits. Although lithographically induced self assembly may not have appeared in my samples, the variegated and attractive patterns which did form created opportunities for a great deal of interesting theory and research. Perhaps some interested student of microfabrication or polymer thin films will choose to continue my research, to determine how the patterns change with time, heat, electricity, try and discover practical uses for these intriguing phenomena, or simply find just the right conditions for LISA to occur. I wish them luck.

9 Bibliography

References

[1] S. Y. Chou and L. Zhuang. "Lithographically induced self-assembly of periodic polymer micropillar arrays." J. Vac. Sci. Technol. B **17**(6), 3197 (Nov. 1999)

[2] S. Y. Chou, L. Zhuang, and L. Guo. "Lithographically induced self-construction of polymer microstructures for resistless patterning." Appl. Phys. Lett. **75**(7), 1004 (16 Aug 1999)

[3] S. Y. Chou et al. "Sub-10 nm imprint lithography and applications." J. Vac. Sci. Tech. B 15(6), 2897 (Nov 1997)

[4] S.Y. Chou, P. R. Krauss, and P. J. Renstrom. "Imprint of sub-25 nm vias and trenches in polymers." App. Phys. Lett. **67**(21), 3114 (20 November 1995)

[5] S.Y. Chou, P. R. Krauss, and P. J. Renstrom. "Nanoimprint lithography." J. Vac. Sci. Tech. **14**(6), 4129 (Nov/Dec 1996)

[6] P. Deshpande, X. Sun, S. Y. Chou. "Observation of dynamic behavior of lithographically induced self-assembly of supramolecular periodic pillar arrays in a homopolymer film." App. Phys. Lett. **79**(11), 1688 (10 September 2001)

[7] P. Deshpande and S. Y. Chou. "Lithographically induced self-assembly of microstructures with a liquid-filled gap between the mask and polymer surface." J. Vac. Sci. Tech. B **19**(6), 2741 (November 2001)

[8] S. Herminghaus et al. "Liquid microstructures at solid interfaces." J. Phys. Condens. Matt. **12**, A57 (2000)

[9] X. Lei et al. "100 nm period gratings produced by lithographically induced self-construction." Nanotechnology **14**, 786 (May 2003)

[10] H. Li and W. T. S. Huck. "Polymers in nanotechnology." Current Opinion in Solid State and Materials Science **6**, 3 (2003)

[11] Lu, Yunfeng et al., eds. Self-Assembled Nanostructured Materials (Materials Research Society Symposium Proceedings Vol. 775) Materials Research Society, Warrendale, PA. 2003.

[12] Müller-Buschbaum, P. "Dewetting and pattern formation in thin polymer films as investigated in real and reciprocal space." J. Phys. Condens. Matt. **15** R1549 (2003)

[13] E. Schäffer, T. Thurn-Albrecht, T. P. Russell and U. Steiner. "Electrically induced structure formation and pattern transfer." Letters to Nature **403**, 874-877 (24 February 2000.)

[14] E. Schäffer, Z. Lin et al. "Electric field induced instabilities at liquid-liquid interfaces." J. Chem. Phys. **114**(5), 2377-2381 (1 February 2001)

[15] E. Schäffer, T. Thurn-Albrecht, T. P. Russell and U. Steiner. "Electrohydrodynamic instabilities in polymer films." Europhys. Lett. **53**(4), 518-524 (15 February 2001)

[16] H. Schift et al. "Pattern formation in hot embossing of thin polymer films." Nanotechnology **12**, 173 (2001)

[17] Z. Suo and J. Liang. "Theory of lithographically-induced self-assembly." App. Phys. Lett.**78**(25), 3971 (18 June 2001)

[18] L. Wu and S. Y. Chou. "Dynamic modeling and scaling of nanostructure formation in the lithographically induced self-assembly and self-construction." App. Phys. Lett. **82**(19), 3200 (12 May 2003)

[19] Jones, Richard A. L. Soft Condensed Matter. Oxford University Press, New York, 2002.

10 Appendix One: A Selection of Interesting Images

Over the course of the semester, I amassed quite a large collection of AFM images of the polymer structures. Although the images in the text serve to illustrate the theory and results of this project particularly well, I felt that many of the other pictures were also worthy of inclusion, illustrating particularly interesting, unexplained or simply beautiful phenomena.

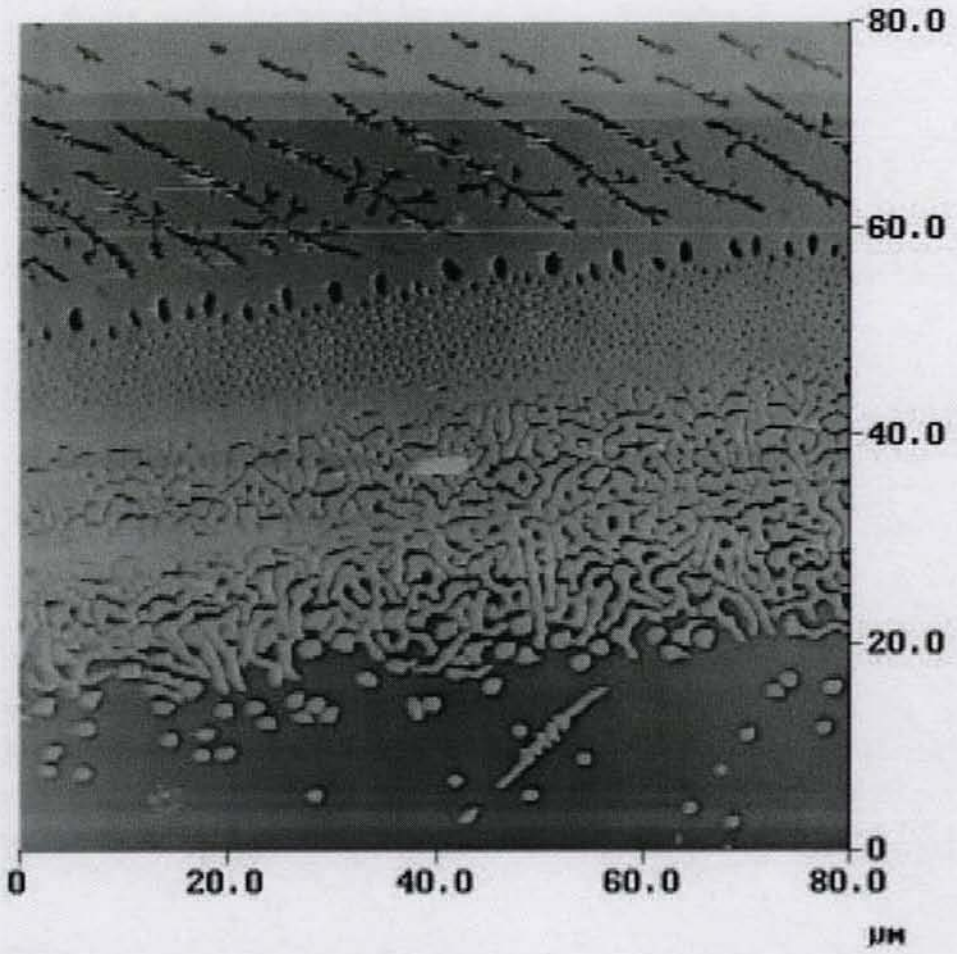

Figure 18: A thin line of patterning showing a variety of different forms and the transitions between them.

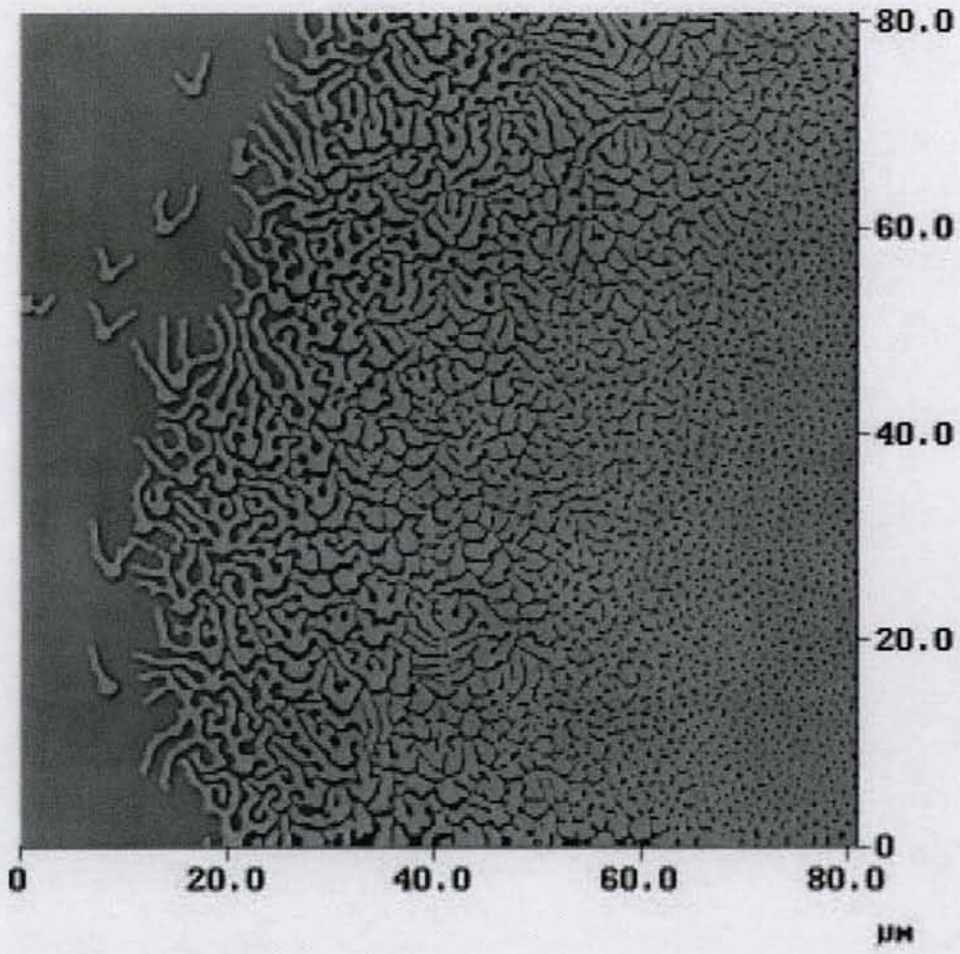

Figure 19: Another image of a transitional area. The V-shaped features to the left are particularly interesting.

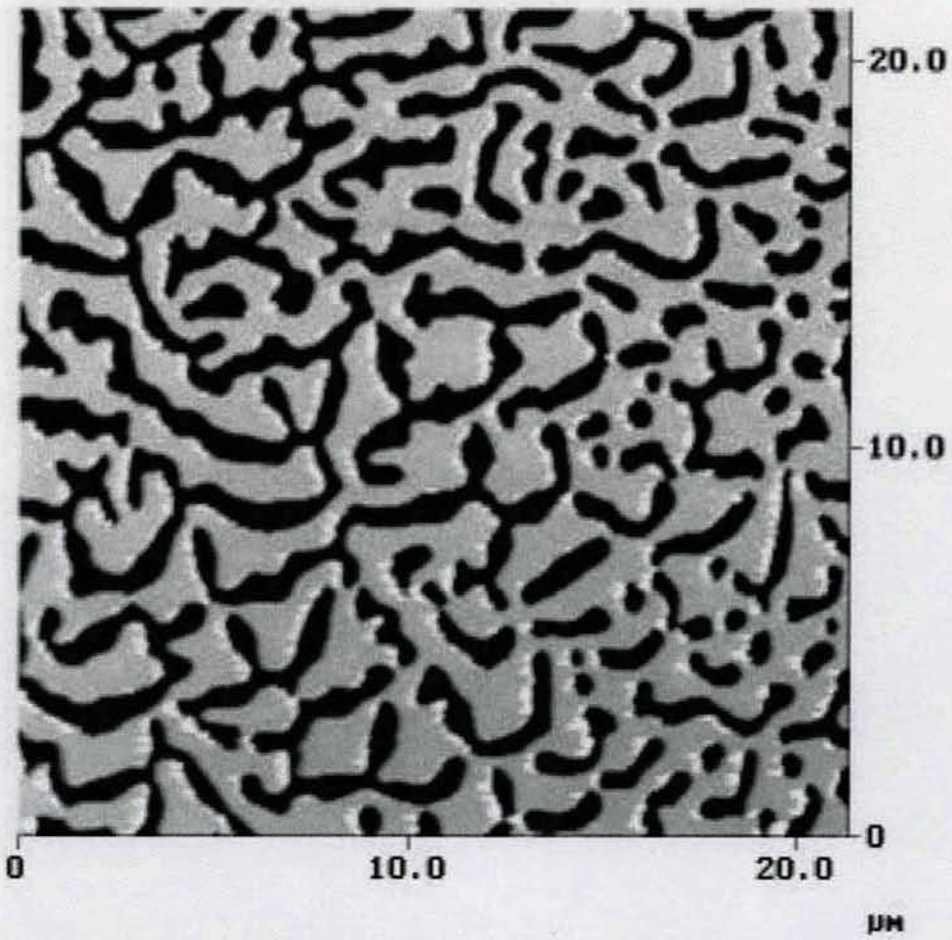

Figure 20: A "negative labyrinth" area.

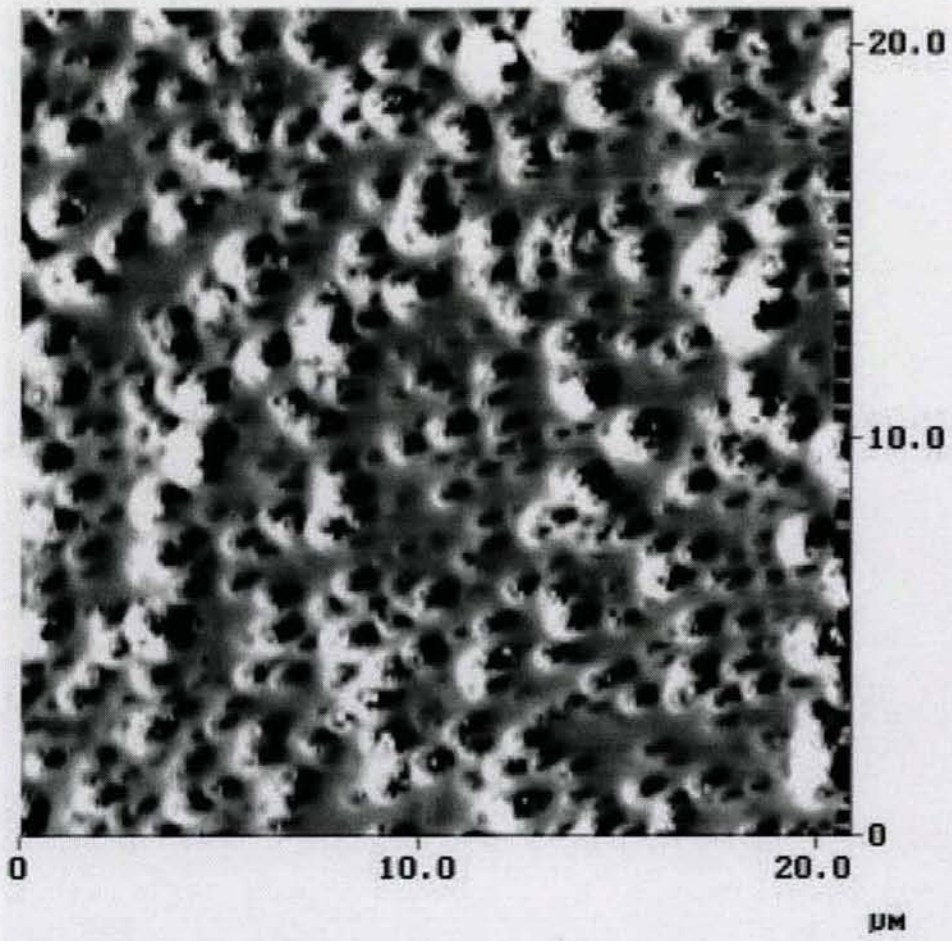

Figure 21: An area of highly varied, irregular topography

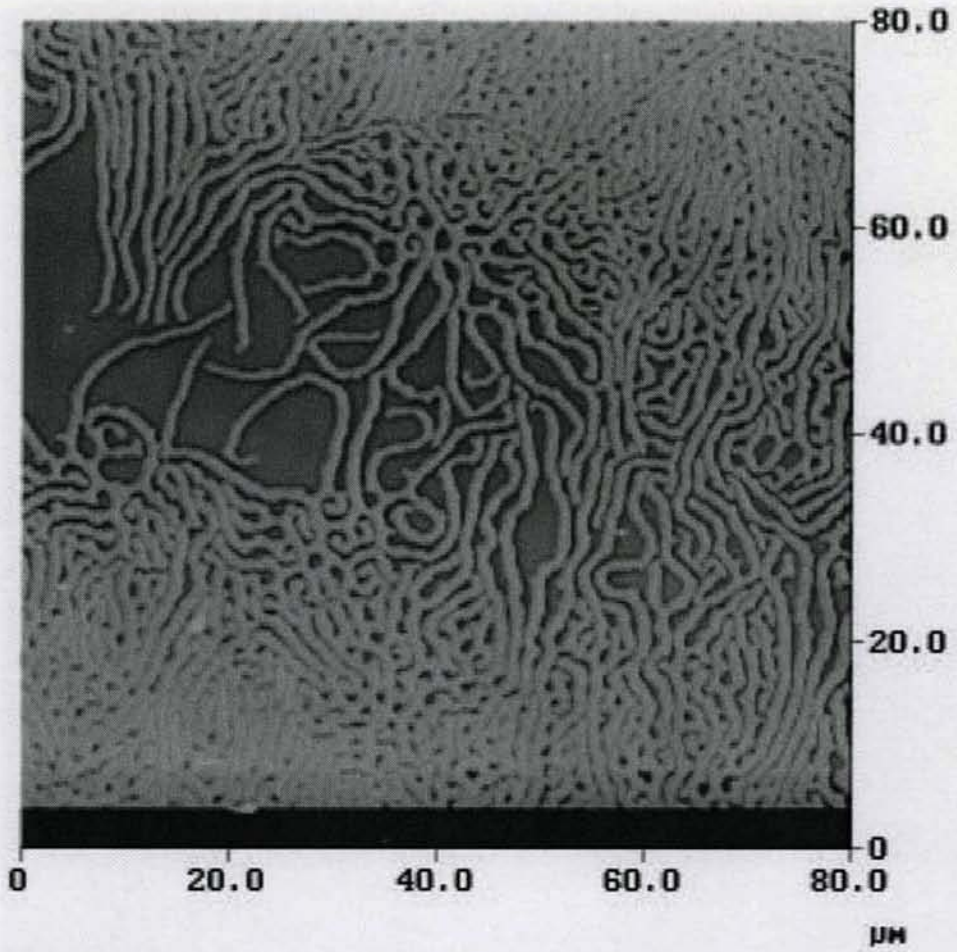

Figure 22: "Tendrils" in the spinodal decomposition phase reach across a gap.

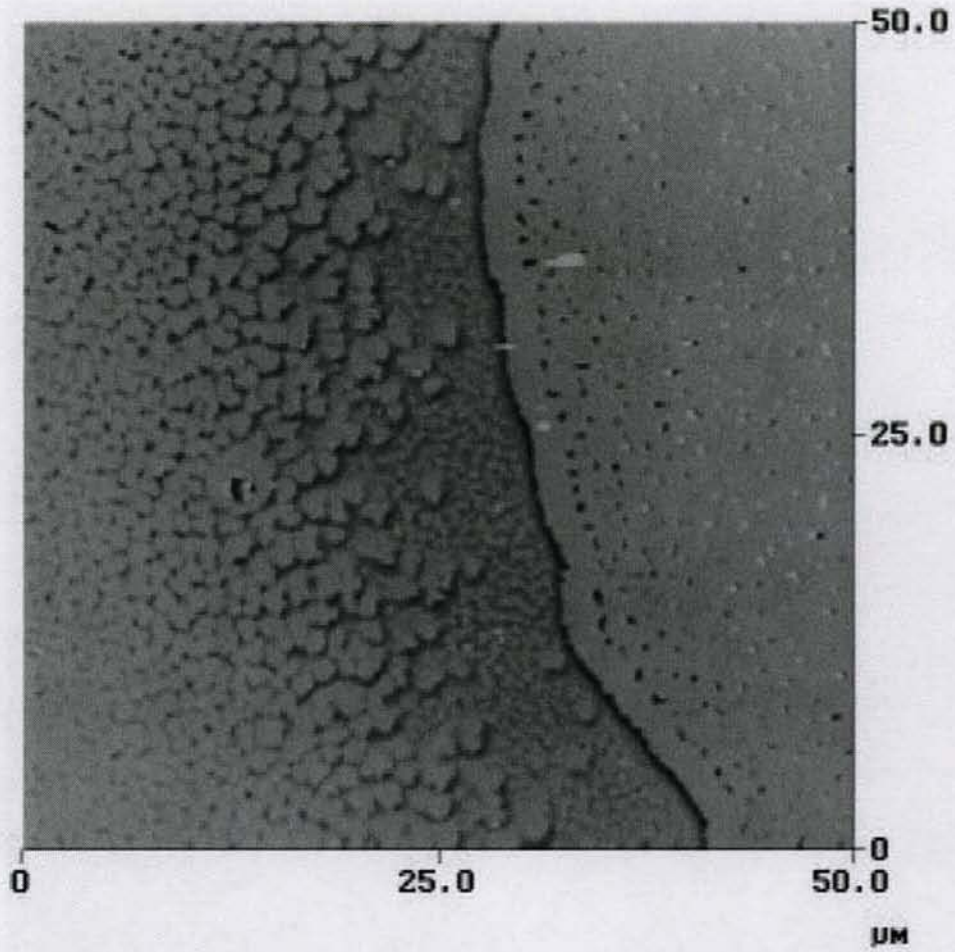

Figure 23: An abrupt transition from one phase to another—holes to pillars and back again.